AIAA JOURNAL
Vol. 41, No. 5, May 2003

Analysis of Sandwich Plates with Viscoelastic Damping Using Two-Dimensional Plate Modes

Gang Wang* and Norman M. Wereley†
University of Maryland, College Park, Maryland 20742
and
Der-Chen Chang‡
Georgetown University, Washington, D.C. 20057

A higher-order assumed modes analysis for a sandwich plate is developed. The base plate is an isotropic plate with the parallel edges of its span clamped and with its remaining edges free. An isotropic constraining layer sandwiching a viscoelastic core is centrally located over one-third of the span across the plate's chord. Analysis of the base plate uses two-dimensional plate bending and in-plane extension mode shapes based on the Kantorovich–Krylov method. Free–free one-dimensional rod modes are used to approximate in-plane motions in both x and y directions for the constraining plate, and bending displacement compatibility is assumed between base and constraining plates. The Golla–Hughes–McTavish method was used to account for the frequency-dependent complex shear modulus of the viscoelastic core. Natural frequencies, mode shape functions, loss factors, and frequency responses of the sandwich plate were calculated and compared to the results of our previous analysis using one-dimensional beam and rod modes. Fewer modes were needed in the current analysis to achieve the same accuracy as compared to the previous analysis. Experiments were conducted to validate predictions, and the experimental data substantially agree with our results.

Nomenclature

E	=	Young's modulus of plate material
G^*	=	complex modulus of viscoelastic core, $G' + jG''$
h_i	=	plate thickness in each layer, $i = 1, 2, 3$
$M_{x,i}$	=	bending moment of base or constraining plate in x direction, $i = 1, 3$
$M_{y,i}$	=	bending moment of base or constraining plate in y direction, $i = 1, 3$
$M_{xy,i}$	=	twist moment of base or constraining plate, $i = 1, 3$
$N_{x,i}$	=	in-plane normal stress of base or constraining plate in x direction, $i = 1, 3$
$N_{y,i}$	=	in-plane normal stress of base or constraining plate in y direction, $i = 1, 3$
$N_{xy,i}$	=	in-plane shear stress of base or constraining plate, $i = 1, 3$
$Q_{x,2}$	=	shear stress of viscoelastic core in x direction
$Q_{y,2}$	=	shear stress of viscoelastic core in y direction
$u_1(x, y, t)$	=	in-plane displacement of base plate in x direction
$u_3(x, y, t)$	=	in-plane displacement of constraining plate in x direction
$v_1(x, y, t)$	=	in-plane displacement of base plate in y direction
$v_3(x, y, t)$	=	in-plane displacement of constraining plate in y direction
$w(x, y, t)$	=	bending displacement of base plate
$\gamma_{x,2}$	=	shear strain of viscoelastic core in x direction
$\gamma_{y,2}$	=	shear strain of viscoelastic core in y direction
ν	=	Poisson's ratio of base and constraining plates
ρ_i	=	density of each layer in a sandwich plate, $i = 1, 2, 3$
$\Phi^i_{u_1}(x, y)$	=	ith in-plane mode shape of displacement u_1
$\Phi^i_{u_3}(x, y)$	=	ith in-plane mode shape of displacement u_3
$\Phi^i_{v_1}(x, y)$	=	ith in-plane mode shape of displacement v_1
$\Phi^i_{v_3}(x, y)$	=	ith in-plane mode shape of displacement v_3
$\Phi^i_w(x, y)$	=	ith bending mode shape of displacement w

Introduction

SINCE the 1950s, many papers have discussed the modeling and analysis of sandwich plates with a viscoelastic core. Ross et al.[1] studied simply supported plates and assumed a perfect interface and compatibility of transverse displacement in each layer. Rao and Nakra[2] developed the basic equations of vibratory bending of asymmetric sandwich plates with isotropic face plates and a viscoelastic core. Cupial and Niziol[3] used the variational method to model sandwich plates with anisotropic face plates and presented simplified forms of the equations for a symmetric plate or for specially orthotropic face layers. The cited theories laid the foundation for the analysis of sandwich plates. However, an effective and accurate way to solve these problems numerically is needed. In previous work,[4] the Galerkin assumed modes method was successfully applied, in conjunction with the method of Golla–Hughes–McTavish (GHM) (see Ref. 5), to the analysis of sandwich plates with isotropic face plates and a viscoelastic core using one-dimensional beam and rod mode shapes. We considered sandwich plates fully treated with passive constrained layer damping (PCLD), under clamped boundary condition along all four sides. The plate mode shape functions were approximated by one-dimensional beam and rod modes in both x and y directions to have admissible functions that satisfy the geometric boundary conditions. The modal frequencies were calculated and validated experimentally. However, a large number of mode shapes, especially in-plane plate mode shapes, were needed to achieve acceptable accuracy in comparison with experimental

Presented as Paper 2002-1366 at the AIAA/ASME/ASCE/AHS/ASC 43rd Structures, Structural Dynamics, and Materials Conference, Denver, CO, 22–25 April 2002; received 26 June 2002; revision received 7 January 2003; accepted for publication 10 January 2003.

*Research Associate, Smart Structures Laboratory, Alfred Gessow Rotorcraft Center, Department of Aerospace Engineering; gwang@eng.umd.edu. Member AIAA.

†Associate Professor of Aerospace Engineering, Smart Structures Laboratory, Alfred Gessow Rotorcraft Center, Department of Aerospace Engineering; wereley@eng.umd.edu. Associate Fellow AIAA.

‡Professor and Director, Mathematical Sciences Center, Department of Mathematics; chang@georgetown.edu.

data. Moreover, both modal frequencies and frequency-response functions are needed to assess performance of sandwich structures in engineering applications. The GHM or similar method must be used to account for the frequency-dependent complex shear modulus of the viscoelastic core. The additional dissipation coordinates used in the GHM method substantially increase the degrees of freedom in the analysis. To calculate the natural frequencies of sandwich plate structures, a large-order eigenvalue problem must be solved.

Our objective is to alleviate the computational cost in these analyses by using fewer assumed mode shapes. It is very difficult to solve analytically the two-dimensional boundary value problems for rectangular sandwich plates. Closed-form solutions exist only for a sandwich plate with simply supported boundary conditions, as described by Cupial and Niziol.[3] However, free and clamped boundary conditions are often encountered in practical engineering applications. Alternatively, we will update assumed modes analysis by using two-dimensional plate mode shape functions therein. We observe that the shear deformation in the viscoelastic core causes the coupling between the bending and in-plane motions in both the base and constraining plates for a sandwich plate system. Therefore, accurate representations of the two-dimensional plate bending and in-plane mode shape functions would improve our assumed modes for sandwich plate analysis. Usually, for isotropic rectangular thin plates, the bending and in-plane vibrations are uncoupled under the Kirchhoff hypothesis, as shown by Doyle.[6] The biharmonic and Navier's equations correspond to the governing equations of bending and in-plane vibrations of a rectangular plate, respectively. The next question is how to obtain these two-dimensional plate mode shape functions for bending and in-plane vibrations of isotropic rectangular plates.

For the bending vibration, the closed-form solutions exist only for the Levy type of plate that is at least two parallel edges with simply supported boundary conditions (see Ref. 7). The Levy-type plate has an exact solution, and the displacement can be determined using separation of variables, which reduces the plate problem to a beamlike one-dimensional problem. Similarly, for rectangular plate in-plane vibration, exact solutions exist only for the case of four sides with simply supported boundary conditions.[8] For other types of boundary conditions, there is no separable solution form, as is usually assumed. We need to determine the mode shape functions for plates with free and clamped boundary conditions because they are commonly encountered in practical engineering applications.

Fortunately, the Kantorovich–Krylov method[9] can provide a higher-order solution for plate bending and in-plane vibration using a single separable term. This method was based on the variational principle where the equilibrium position of a mechanical system is the position corresponding to the minimum potential energy. Solutions of the boundary value problem for partial differential equations (PDEs) is equivalent to the problem of finding the function minimizing the integral of total potential energy. This equivalence enables us to solve PDEs by minimizing the total energy. The most familiar method using this principle is the Rayleigh–Ritz method (see Refs. 10 and 11). This method provides only approximate solutions of PDEs because the assumed mode shapes are only admissible functions. The Galerkin method can provide exact solutions for PDEs, but it is very difficult to find functions, a priori, that satisfy both geometric and force boundary conditions for all cases. However, the Kantorovich–Krylov variational method[9] can reduce PDEs to ordinary differential equations (ODEs), so that we can solve these ODEs to determine the mode shape functions analytically. An iteration scheme is developed to calculate the modal frequencies and coefficients of the corresponding mode shape functions. Bhat et al.[12] solved plate bending mode shapes for boundary conditions of combinations of simply supported and clamped cases. We apply the same method to solve for out-of-plane (bending) plate mode shapes with free or clamped boundary conditions. The analytical expressions for bending mode shapes are described in Ref. 13.

On the other hand, few papers discuss mode shapes of in-plane plate vibration. We extended the Kantorovich–Krylov method[9] to in-plane plate vibration problems.[14,15] The predictions of natural frequency of in-plane plate vibration were analytically validated by

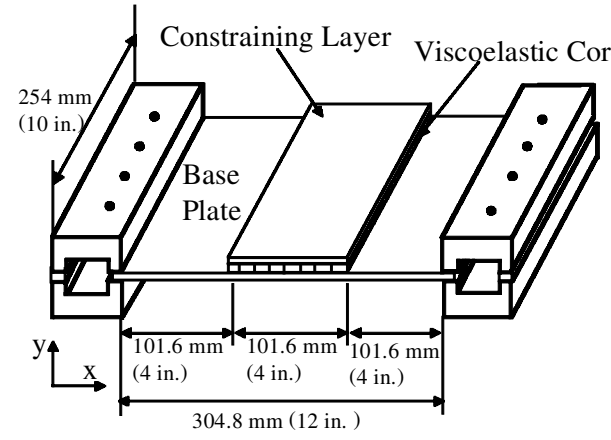

Fig. 1 Plate with partially passive damping treatment under CFCF boundary conditions.

NASTRAN and other results from the literature.[16] Then, these two-dimensional plate bending and in-plane mode shapes were employed in the analysis of sandwich plates using the assumed modes method, in which the GHM method was used to account for the frequency-dependent complex shear modulus of the viscoelastic core.

In this paper, we consider a plate with a partial PCLD treatment, as shown in Fig. 1. The base plate was clamped along two parallel edges in the x direction, with free edges along the y direction, that is, clamped–free–clamped–free (CFCF) boundary conditions. The plate was 304.8 mm (12 in.) long, 254 mm (10 in.) wide, and 1.5177 mm (0.05975 in.) thick. The passive constrained layer damping treatment was located in the center of the base plate, which covered one-third span of the base plate and the entire chord. The thickness of the constraining plate was 0.3969 mm (1/64 in.), and the viscoelastic core was 0.0508 mm (2 mil) thick. We developed a higher-order assumed modes method for the sandwich plate analysis. The two-dimensional plate bending and in-plane mode shape functions, which were determined using the Kantorovich–Krylov method,[9] were assumed for the base plate motion. In contrast, one-dimensional rod modes were assumed for in-plane motion of the constraining plate to decrease the number of modes involved. We assumed that the bending displacement is compatible between base and constraining plates. Again, the GHM method was used to account for the frequency-dependent properties of the viscoelastic core. Fewer modes are needed to achieve the same accuracy as achieved by our previous assumed modes method, in which one-dimensional beam and rod modes were used to approximate the two-dimensional plate bending and in-plane modes, respectively, in both x and y directions. The predictions of frequency, mode shape functions, loss factor, and frequency response are validated experimentally. We will describe and assess the accuracy of our proposed method and compare it to the assumed analysis based solely on one-dimensional assumed modes.

Analysis of Sandwich Plate

As shown in Fig. 1, a plate with partial PCLD treatment was investigated. The base plate is an isotropic aluminum plate under CFCF boundary conditions. A centrally located PCLD patch covers one-third of the span and covers the chord of the base plate. To analyze this sandwich, we have to consider two regions. The first region is the base plate without PCLD treatment, which is an isotropic rectangular plate. The Navier and biharmonic equations can be used to describe the dynamics of in-plane and out-of-plane (bending) vibrations,[6] respectively. The second region is the base plate with PCLD treatment, which is a three-layered sandwich plate structure. Once we have governing PDEs for the two regions, we could try to solve them by applying the appropriate boundary conditions and compatibility conditions along the junctions. However, it is not practical to solve such a two-dimensional boundary value problem for sandwich plate structures. Therefore, we resort to the assumed modes method (Ritz method) (see Refs. 10 and 11).

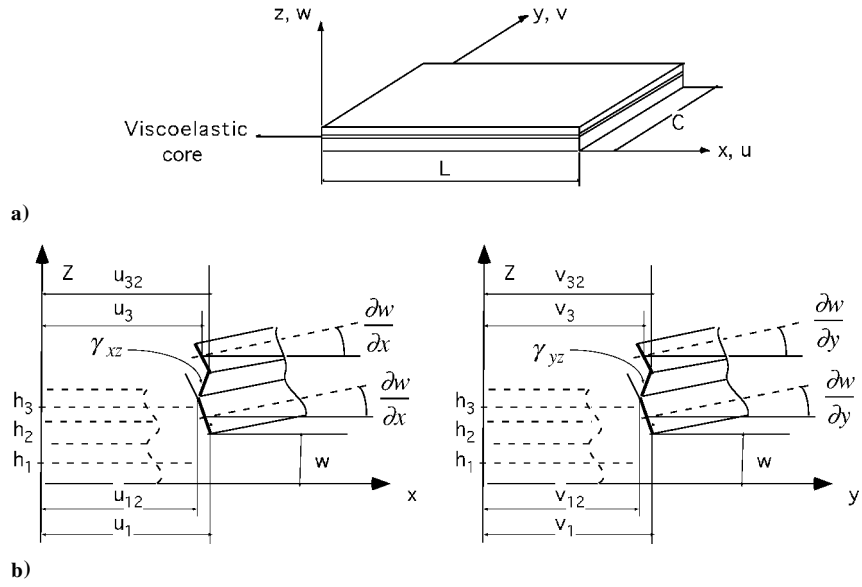

Fig. 2 Sandwich plate and layer displacements: a) coordinate axes and dimensions and b) layers forming sandwich.

In previous analysis,[4] one-dimensional beam and rod modes were used to approximate two-dimensional plate modes in the assumed modes method. The displacements were assumed to be an expansion of plate mode shapes with unknown coefficients. These coefficients were determined by second-order ODEs when these assumed plate mode shapes were applied to the system energy expression. In this paper, we propose an approach to improve the assumed modes method by using two-dimensional plate mode shapes, which are determined using the Kantorovich–Krylov method[9] (also see Ref. 13). We expect to save computational cost compared to the previous method,[4] in which one-dimensional beam and rod mode shapes were used. Also the GHM method was used to account for the frequency-dependent complex shear modulus of viscoelastic core in both cases. We will first derive the governing equations of a plate with PCLD treatment and then present our solution approach.

Governing Equations of a Plate with PCLD Treatment

The configuration of three-layered sandwich plate is shown in Fig. 2. Layers 1 and 3 are the isotropic face plates, made from aluminum, and the core is the viscoelastic material. The face plates are assumed to have bending, in-plane shear, and extensional stiffness, and their rotatory inertia has also been neglected in the model. The viscoelastic core is assumed to have transverse shear stiffness alone.

The shear strain in the viscoelastic core (layer 2) can be expressed by

$$\gamma_{x,2} = \frac{u_{32} - u_{12}}{h_2} + \frac{\partial w}{\partial x} = \frac{u_3 - u_1}{h_2} + \frac{d}{h_2}\frac{\partial w}{\partial x}$$

$$\gamma_{y,2} = \frac{v_{32} - v_{12}}{h_2} + \frac{\partial w}{\partial y} = \frac{v_3 - v_1}{h_2} + \frac{d}{h_2}\frac{\partial w}{\partial y} \tag{1}$$

where d is the distance between the midplane of layer 1 and midplane of layer 3 and is defined as

$$d = h_2 + (h_1 + h_3)/2 \tag{2}$$

To derive the governing equations, we can write the total kinetic and potential energies in terms of five displacements: in-plane displacement in face layer 1, $u_1(x, y, t)$ and $v_1(x, y, t)$; in-plane displacement in face layer 3, $u_3(x, y, t)$ and $v_3(x, y, t)$; and transverse displacement $w(x, y, t)$ for whole sandwich plate. The kinetic energy of sandwich plate is

$$T = \frac{1}{2}\int_A \left\{ \rho h \left(\frac{\partial w}{\partial t}\right)^2 + \sum_{i=1,3} \rho_i h_i \left[\left(\frac{\partial u_i}{\partial t}\right)^2 + \left(\frac{\partial v_i}{\partial t}\right)^2 \right] \right\} \mathrm{d}A \tag{3}$$

The mass per unit area for a total sandwich plate is defined as

$$\rho h = \rho_1 h_1 + \rho_2 h_2 + \rho_3 h_3 \tag{4}$$

The total potential energy of sandwich plate, including the transverse bending, in-plane energy in the face layers 1 and 3, and the transverse shear energy alone in the core, is

$$U = \frac{1}{2}\int_A \left[\sum_{i=1,3} N_{x,i}\frac{\partial u_i}{\partial x} + \sum_{i=1,3} N_{y,i}\frac{\partial v_i}{\partial y} + \sum_{i=1,3} N_{xy,i}\left(\frac{\partial u_i}{\partial y} + \frac{\partial v_i}{\partial x}\right) - \sum_{i=1,3} M_{x,i}\frac{\partial^2 w}{\partial x^2} - \sum_{i=1,3} M_{y,i}\frac{\partial^2 w}{\partial y^2} - 2\sum_{i=1,3} M_{xy,i}\frac{\partial^2 w}{\partial x \partial y} + \bar{Q}_{x,2}\gamma_{x,2} + \bar{Q}_{y,2}\gamma_{y,2} \right] \mathrm{d}A \tag{5}$$

In layers 1 and 3, the resultant in-plane stresses are

$$N_{x,i} = \int_{-h_i/2}^{h_i/2} \sigma_{x,i}\,\mathrm{d}z = \frac{E_i h_i}{1-\nu^2}\left(\frac{\partial u_i}{\partial x} + \nu\frac{\partial v_i}{\partial y}\right)$$

$$N_{y,i} = \int_{-h_i/2}^{h_i/2} \sigma_{y,i}\,\mathrm{d}z = \frac{E_i h_i}{1-\nu^2}\left(\frac{\partial v_i}{\partial y} + \nu\frac{\partial u_i}{\partial x}\right)$$

$$N_{xy,i} = \int_{-h_i/2}^{h_i/2} \sigma_{xy,i}\,\mathrm{d}z = \frac{E_i h_i}{2(1+\nu)}\left(\frac{\partial u_i}{\partial y} + \frac{\partial v_i}{\partial x}\right) \qquad i = 1, 3 \tag{6}$$

bending moments are defined as

$$M_{x,i} = \int_{-h_i/2}^{h_i/2} \sigma_{x,i} z\,\mathrm{d}z = -\frac{E_i h_i^3}{12(1-\nu^2)}\left(\frac{\partial^2 w}{\partial x^2} + \nu\frac{\partial^2 w}{\partial y^2}\right)$$

$$M_{y,i} = \int_{-h_i/2}^{h_i/2} \sigma_{y,i} z\,\mathrm{d}z = -\frac{E_i h_i^3}{12(1-\nu^2)}\left(\frac{\partial^2 w}{\partial y^2} + \nu\frac{\partial^2 w}{\partial x^2}\right)$$

$$M_{xy,i} = \int_{-h_i/2}^{h_i/2} \sigma_{xy,i} z\,\mathrm{d}z = -\frac{E_i h_i^3}{12(1+\nu)}\left(\frac{\partial^2 w}{\partial x \partial y}\right) \qquad i = 1, 3 \tag{7}$$

and shear stresses in the viscoelastic core are

$$\bar{Q}_{x,2} = G\int_{-h_2/2}^{h_2/2} \sigma_{xz,2}\,\mathrm{d}z = Gh_2\left(\frac{u_3 - u_1}{h_2} + \frac{d}{h_2}\frac{\partial w}{\partial x}\right)$$

$$\bar{Q}_{y,2} = G\int_{-h_2/2}^{h_2/2} \sigma_{yz,2}\,\mathrm{d}z = Gh_2\left(\frac{v_3 - v_1}{h_2} + \frac{d}{h_2}\frac{\partial w}{\partial y}\right) \tag{8}$$

G will be replaced by the complex shear modulus G^* in the governing equations later. The complex shear modulus G^* is composed of two components, the in-phase (real) part G' and quadrature (imaginary) part G'', which are defined in the frequency domain. However, the total energy of a sandwich plate will be a complex number if we introduce the complex shear modulus G^* into the expression directly. This does not make sense physically. Therefore, we use the real component of shear modulus, $G = G'$, in our derivation and replace it by the complex shear modulus, using the correspondence principles,[17] after the governing equation of motion has been derived. To represent the complex shear modulus in the time domain, an additional damping model must be introduced to capture the time-domain behavior of viscoelastic materials, for example, the GHM method.

Using the Hamiltonian principle, we obtain the governing equations and boundary conditions. There are five partial differential equations corresponding to five independent displacements. Next, we introduce the complex shear modulus of viscoelastic core G^* in place of G'. We present the equations in terms of five displacements: in-plane displacement in face layer 1, $u_1(x, y, t)$ and $v_1(x, y, t)$; in-plane displacement in face layer 3, $u_3(x, y, t)$ and $v_3(x, y, t)$; and transverse displacement $w(x, y, t)$ for the entire sandwich plate:

$$\rho h \frac{\partial^2 w}{\partial t^2} + D_t \left[\frac{\partial^4 w}{\partial x^4} + 2\frac{\partial^4 w}{\partial x^2 \partial y^2} + \frac{\partial^4 w}{\partial^4 y} \right] = \frac{d}{h_2}\frac{\partial Q_{x,2}}{\partial x} + \frac{d}{h_2}\frac{\partial Q_{y,2}}{\partial y} \tag{9}$$

$$\rho_1 h_1 \frac{\partial^2 u_1}{\partial t^2} - \frac{E h_1}{1-\nu^2}\left[\frac{\partial^2 u_1}{\partial x^2} + \frac{1}{2}(1-\nu)\frac{\partial^2 u_1}{\partial y^2} + \frac{1}{2}(1+\nu)\frac{\partial^2 v_1}{\partial x \partial y} \right] = \frac{Q_{x,2}}{h_2} \tag{10}$$

$$\rho_1 h_1 \frac{\partial^2 v_1}{\partial t^2} - \frac{E h_1}{1-\nu^2}\left[\frac{\partial^2 v_1}{\partial y^2} + \frac{1}{2}(1-\nu)\frac{\partial^2 v_1}{\partial x^2} + \frac{1}{2}(1+\nu)\frac{\partial^2 u_1}{\partial x \partial y} \right] = \frac{Q_{y,2}}{h_2} \tag{11}$$

$$\rho_3 h_3 \frac{\partial^2 u_3}{\partial t^2} - \frac{E h_3}{1-\nu^2}\left[\frac{\partial^2 u_3}{\partial x^2} + \frac{1}{2}(1-\nu)\frac{\partial^2 u_3}{\partial y^2} + \frac{1}{2}(1+\nu)\frac{\partial^2 v_3}{\partial x \partial y} \right] = -\frac{Q_{x,2}}{h_2} \tag{12}$$

$$\rho_3 h_3 \frac{\partial^2 v_3}{\partial t^2} - \frac{E h_3}{1-\nu^2}\left[\frac{\partial^2 v_3}{\partial y^2} + \frac{1}{2}(1-\nu)\frac{\partial^2 v_3}{\partial x^2} + \frac{1}{2}(1+\nu)\frac{\partial^2 u_3}{\partial x \partial y} \right] = -\frac{Q_{y,2}}{h_2} \tag{13}$$

Here, the total bending flexural stiffness and shear force in the viscoelastic core are

$$D_t = \frac{E_1 h_1}{12(1-\nu^2)} + \frac{E_3 h_3}{12(1-\nu^2)}$$

$$Q_{x,2} = G^*\left[u_3 - u_1 + d\frac{\partial w}{\partial x} \right]$$

$$Q_{y,2} = G^*\left[v_3 - v_1 + d\frac{\partial w}{\partial y} \right] \tag{14}$$

The governing equations (9–13) are associated with the following possible boundary conditions along the four edges of a rectangular sandwich plate, which were also obtained from the Hamiltonian principle.

At $x = 0$ and L:

$$\delta u_i = 0 \quad \text{or} \quad N_{x,i} = 0, \qquad \delta v_i = 0 \quad \text{or} \quad N_{xy,i} = 0$$

$$\delta w = 0 \quad \text{or} \quad Q_x = 0, \qquad \frac{\delta \partial w}{\partial x} = 0 \quad \text{or} \quad M_x = 0$$

At $y = 0$ and $y = C$:

$$\delta v_i = 0 \quad \text{or} \quad N_{y,i} = 0, \qquad \delta u_i \quad \text{or} \quad N_{xy,i} = 0$$

$$\delta w = 0 \quad \text{or} \quad Q_y = 0, \qquad \frac{\delta \partial w}{\partial y} = 0 \quad \text{or} \quad M_y = 0$$

for $i = 1, 3$, where

$$M_x = M_{x,1} + M_{x,3}, \qquad M_y = M_{y,1} + M_{y,3}$$

$$M_{xy} = M_{xy,1} + M_{xy,3}, \qquad Q_x = \frac{\partial M_x}{\partial x} + 2\frac{\partial M_{xy}}{\partial y} + \frac{d}{h_2}Q_{x,2}$$

$$Q_y = \frac{\partial M_y}{\partial y} + 2\frac{\partial M_{xy}}{\partial x} + \frac{d}{h_2}Q_{y,2} \tag{15}$$

It is not practical to solve analytically the boundary value problem for the three-layered sandwich plate as just posed. Closed-form solutions exist only for the rectangular sandwich plate with simply supported boundary conditions along four sides, as demonstrated by Cupial and Niziol.[3] However, the combination of free and clamped boundary conditions is commonly encountered in practical engineering applications. An efficient and accurate numerical method is needed to evaluate sandwich plate structures to obtain the results of natural frequency, loss factor, and frequency response.

Approach

We have proposed the assumed modes method for sandwich plate analysis,[4] in which the one-dimensional beam and rod modes were used to approximate two-dimensional plate bending and in-plane modes in both x and y directions. Basically, the five displacements for a sandwich plate were assumed as

$$w(x, y, t) = \sum_i W_i(t)\Phi_w^i(x, y)$$

$$u_1(x, y, t) = \sum_i U_i^1(t)\Psi_{u_1}^i(x, y)$$

$$v_1(x, y, t) = \sum_i V_1^i(t)\Psi_{v_1}^i(x, y)$$

$$u_3(x, y, t) = \sum_i U_3^i(t)\Psi_{u_3}^i(x, y)$$

$$v_3(x, y, t) = \sum_i V_3^i(t)\Psi_{v_3}^i(x, y) \tag{16}$$

where the ith mode shape function Φ_w^i, $\Psi_{u_1}^i$, $\Psi_{v_1}^i$, $\Psi_{u_3}^i$, and $\Psi_{v_3}^i$ were approximated by the beam and rod modes in both the x and y directions based on the different boundary conditions. For example, the plate boundary conditions is CFCF, which means the plate is clamped two edges along x direction and free at two edges along the y direction. Then the ith assumed mode shape function Φ_w^i is a product of beam modes in the x and y directions, which is

$$\Phi_w^i(x, y) = \phi_x^m(x)\phi_y^n(y) \tag{17}$$

$\phi_x^m(x)$ is the mth beam mode shape function under clamped–clamped boundary conditions, whereas $\phi_y^n(y)$ is the nth beam mode shape function under free–free boundary conditions. Similarly, the assumed mode shape functions for $\Psi_{u_1}^i$, $\Psi_{v_1}^i$, $\Psi_{u_3}^i$, and $\Psi_{u_3}^i$ can be obtained. We presented the mapping relationship of modal number i and associated numbers m and n in the x and y directions,

respectively. In previous work,[4] the base plate was fully treated with a PCLD patch. Therefore, substituting the assumed mode shape functions for all of the displacements as illustrated in Eq. (16) into the total energy expression in Eqs. (3) and (5) and applying Lagrange's equation, we can obtain the discretized second-order ODE as

$$M\ddot{\boldsymbol{x}} + K_e\boldsymbol{x} + G^*K_v\boldsymbol{x} = F \tag{18}$$

The mass matrix M and stiffness matrices K_e and K_v are described in Ref. 13. We used the GHM method to account for the frequency-dependent complex shear modulus G^*. The details of the method were discussed in previous work.[4,13] A large number of modes, especially in-plane modes, were needed to achieve acceptable accuracy of frequency predictions compared to experimental data.[4] The number of assumed modes plus additional internal dissipation coordinates in the GHM method lead to a large degree-of-freedom model.

A key goal of our study was to reduce computational cost. To achieve this, we sought to improve the choice of mode shapes used in the assumed modes analysis. A key insight can be gleaned from Eqs. (9–13) when we assume that $G^* = 0$. This results in a decoupling of the bending and in-plane vibration equations. This motivated a higher-order method of sandwich plate analysis using the two-dimensional plate bending and in-plane vibration modes from the decoupled plate bending and extension problems in our assumed modes analysis for the sandwich plates. Therefore, obtaining accurate two-dimensional plate vibration modes becomes a key element of sandwich plate analysis. The Kantorovich–Krylov[9] variational method provides a method of determining higher-order solutions for PDEs. This method can reduce PDEs to ODEs, so that we can solve these ODEs to determine the mode shape functions semi-analytically. An iteration scheme was developed to calculate the modal frequencies and coefficients of the corresponding mode shape functions. We applied the Kantorovich–Krylov method for plate bending and in-plane vibration problems (see Refs. 13 and 14). Based on these two-dimensional plate mode shape functions, a new assumed mode method can be developed for sandwich plate analysis. Now, the ith assumed mode shape function Φ_w^i can be expressed as

$$\Phi_w^i(x, y) = \phi_x^i(x)\phi_y^i(y) \tag{19}$$

Compared to Eq. (17), for the ith mode, the corresponding components in both x and y are uniquely determined. For example, in mode $i = 11$, the component ϕ_x and ϕ_y are uniquely determined, and they are different compared to the mode $i = 12$. However, in the case of using one-dimensional beam mode shape functions, the ϕ_x are assumed to be the same in both mode $i = 11$ and $i = 12$. For other displacement mode shape functions, we have similar expressions, as shown in Eq. (19).

The sandwich plate structure used in our study is shown in Fig. 1. The PCLD treatment was placed on the center of the plate, which fully covered the y direction and covered from $x_1 = 101.6$ mm (4 in.) to $x_2 = 203.2$ mm (8 in.) in the x direction, dividing the plate into three regions: region 1, $(x, y) = [0{:}101.6; 0{:}254]$ mm ([0:4; 0:10] in.), is an isotropic aluminum plate; region 2, $(x, y) = [101.6{:}203.2; 0{:}254]$ mm ([4:8; 0:10] in.), is a three-layer sandwich plate; and region 3, $(x, y) = [203.2{:}304.8; 0{:}254]$ mm ([8:12; 0:10] in.), is an isotropic plate. For the base plate, we assumed CFCF boundary conditions, and for the constraining plate assumed free–free–free–free (FFFF) boundary conditions, where FFFF is a plate free along all edges. The assumed modes method was used to analyze the sandwich plate with PCLD treatment, in which the GHM method was adopted to account for the frequency-dependent complex shear modulus of the viscoelastic core. When we calculate the mass and stiffness matrices, we need to integrate for different subdomains.

Two analyses were developed. The first method is an assumed modes method using one-dimensional beam and rod modes (analysis 1). The second method is an assumed modes method using two-dimensional plate bending and in-plane modes for the base plate and one-dimensional rod modes for in-plane modes in constraining layer (analysis 2). The transverse displacement was assumed compatible between the base and constraining plate in both analyses. In analysis 2, our original goal was to replace one-dimensional mode shape functions by two-dimensional in-plane modes for the constraining plate as well. However, the results were not completely satisfactory. The problem appears to be that we need to consider the coupling between displacement mode shapes in the base plate and constraining layer in Eqs. (9–13). Such coupling is neglected in our current analysis 2, and work is continuing on improving this aspect of the analysis.

Experimental Setup

To validate our analyses, experiments were conducted. Figure 3 shows the experimental setup. A shaker was used as the excitation source and was suspended about 381 mm (15 in.) above the plate. The reason for this is to minimize the influence of the shaker on plate motions. If we fix the shaker, there is additional stiffness contribution from the shaker, which will change the properties of the whole system, and this effect is difficult to include in our analysis. Measured natural frequencies of lower modes using an impact hammer were similar to the results under the shaker excitation for an aluminum plate. Therefore, we do not need to include the effects of the shaker in our analysis.

The force output from the shaker was transmitted through a load cell and a rigid rod to the plate, as shown in Fig. 3. The rigid rod was bonded to the surface of plate using M-bond adhesive (Vishay Micro-Measurements, Inc.) and provided a good adhesion between the rod and plate. The size of the rod is about 38.1 mm (1.5 in.) long and 7.9375 mm (5/16 in.) diameter. The load cell provided the magnitude of force input to the plate. When we assemble the whole system, we ensure that the rigid rod is perpendicular to the surface of the plate to introduce a vertical point force only. We normally adjust the rod so that it just touches the surface of the plate by adjusting the length of elastic strings and allow adhesive to fill the gap between the tip of the rod and plate providing a nearly point transverse force input to the plate.

As shown in Fig. 3, our base is an optical table with a vibration isolation system. This isolation workstation is made by Newport

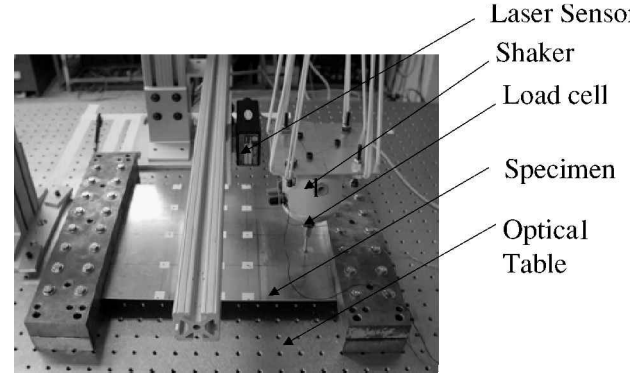

Fig. 3 Photograph of plate testing setup.

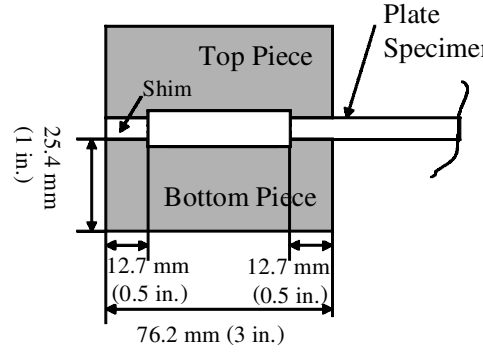

Fig. 4 Diagram of clamping fixture.

Corp. The optical table is Model RS-3000 with integrated tuned damping. The top surface is 400 series ferromagnetic stainless steel with 25.4 mm (1 in.) by 25.4 mm (1 in.) screw pattern; the diameter is 7.9375 mm (5/16 in.). An air compressor serves as the air source to the isolation legs of the workstation system. The isolation system floats the table, and very low-frequency disturbances from the floor were isolated. The details are given by Fowler et al.[18]

A plate was clamped by fixture on two parallel edges and free on the other two edges, as shown in Fig. 4. The fixtures were designed to provide clamped boundary conditions and were made of top and bottom parts. The size of top and bottom parts were the same, 381 mm (15 in.) long, 76.2 mm (3 in.) wide, and 25.4 mm (1 in.) thick. The two bottom pieces were bolted to the optical table at a distance 304.8 mm (12 in.) apart. A 330.2 mm (13 in.) by 254 mm (10 in.) aluminum plate specimen with a thickness of 1.5177 mm (0.05975 in.), was placed on top of the two bottom pieces. The clamping width was a 12.7 mm (0.5 in.) at each clamped edge. A torque of 22.597 N · m (200 lbf · in.) was applied to each of the bolts to provide uniform clamping. Figure 4 shows the details of the clamping fixture.

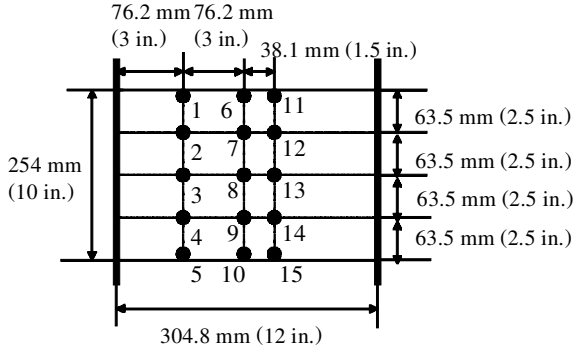

Fig. 5 Schematic of sensor array for plate testing.

The plate with PCLD was 304.8 mm (12 in.) long and 254 mm (10 in.) wide, and the base plate thickness was 1.5177 mm (0.05975 in.) The constraining plate layer was 101.6 mm (4 in.) long, 254 mm (10 in.) wide, and 0.381 mm (0.015 in.) thick. The viscoelastic core is 3M ISD112 (Ref. 19) with 0.0508-mm (2-mil) thickness. The PCLD treatment was located on the center of base plate, which was from $x_1 = 101.6$ mm (4 in.) to $x_2 = 203.2$ mm (8 in.), as shown in Figure 1. The base aluminum plate was 6061T6 with the Young's modulus $E = 68$ GPa and Poisson's ratio $\nu = 0.3$. As shown in Fig. 3, a noncontact Schaevitz Distance Star laser sensor was used to measure plate displacement. We obtained a frequency-response function at 15 positions on the plate. A schematic of the sensor array for plate testing is given in Fig. 5. The coordinates of the measurements for our specimen are listed in Table 1.

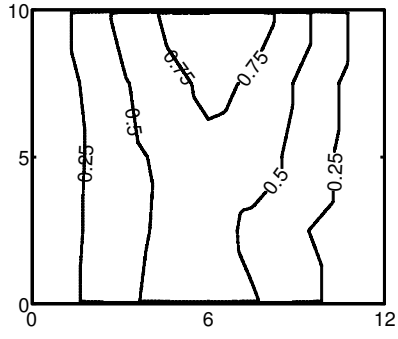

a) Mode (1, 1), ω = 83.1 Hz

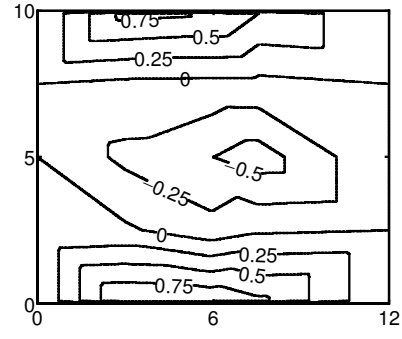

c) Mode (1, 3), ω = 218.9 Hz

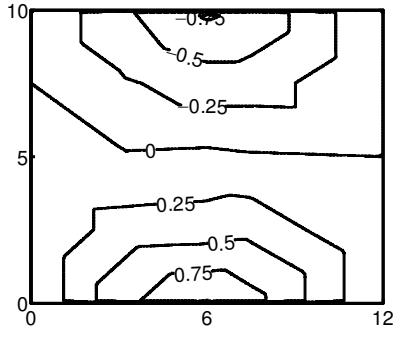

b) Mode (1, 2), ω = 104.91 Hz

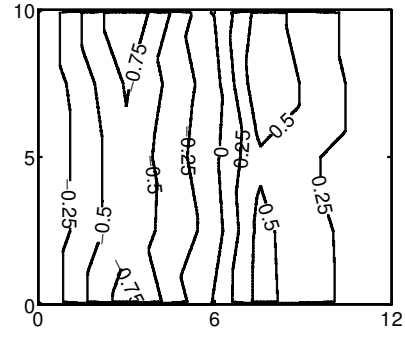

d) Mode (2, 1), ω = 234.2 Hz

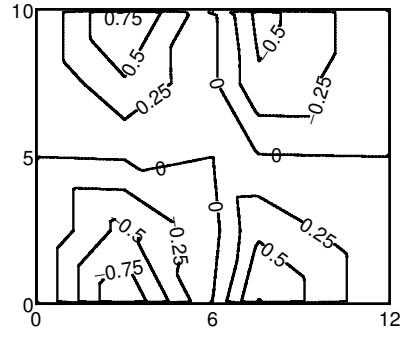

e) Mode (2, 2), ω = 277.8 Hz

Fig. 6 Contour plot of experimental bending mode shape functions for plate with PCLD treatment under CFCF boundary conditions.

Table 1 Coordinates of the 15 measured locations for a plate with PCLD treatment under CFCF boundary conditions

	Coordinate values, mm, at location:														
Coordinate	1	2	3	4	5	6	7	8	9	10	11	12	13	14	15
x	76.2	76.2	76.2	75.41	74.61	152.4	152.4	152.4	150.81	149.22	192.09	191.29	191.29	190.5	190.5
y	252.42	190.5	127	63.5	1.59	250.83	189.71	127	63.5	2.38	251.62	190.5	127	63.5	0.79

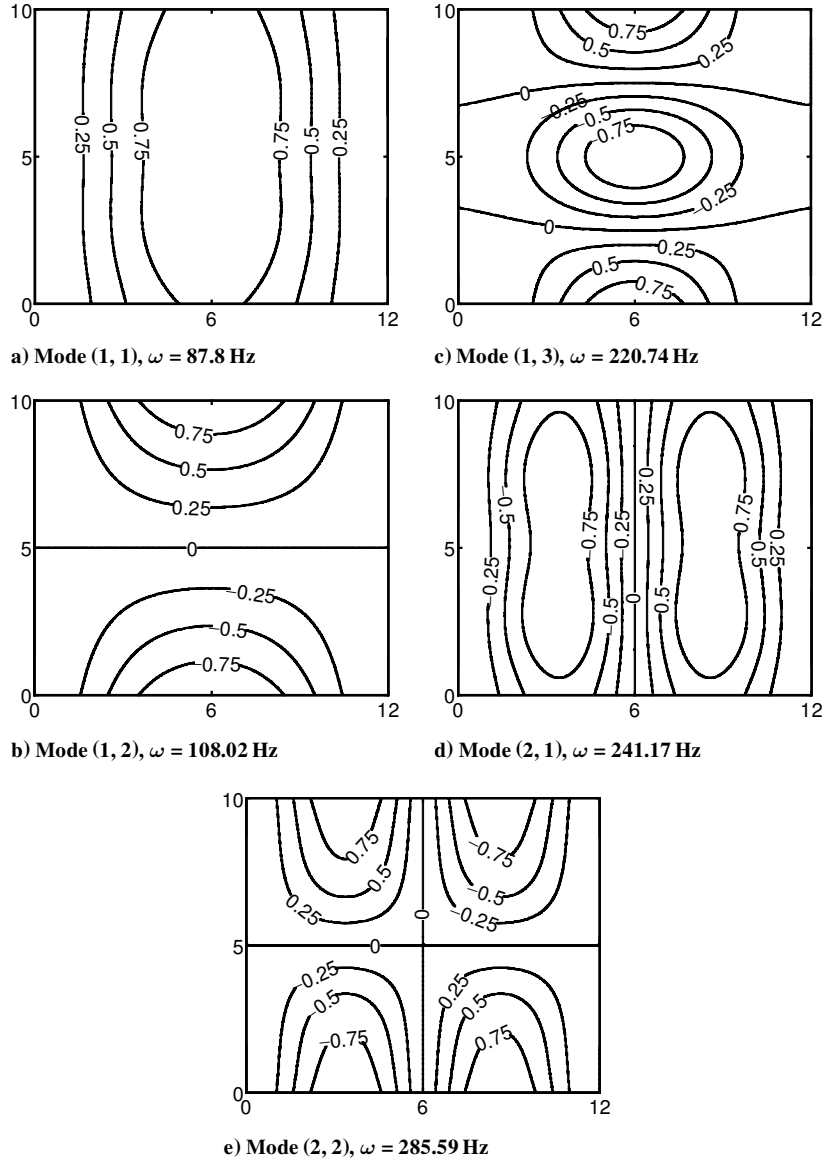

a) Mode (1, 1), ω = 87.8 Hz

c) Mode (1, 3), ω = 220.74 Hz

b) Mode (1, 2), ω = 108.02 Hz

d) Mode (2, 1), ω = 241.17 Hz

e) Mode (2, 2), ω = 285.59 Hz

Fig. 7 Contour plot of analytical bending mode shape functions for plate with PCLD treatment under CFCF boundary conditions.

We chose the excitation location carefully to avoid exciting at nodal lines of the plates. We draw the lines that equally divided the length in both the x and y directions. Then, we can find the location that can excite up to fourth mode in each direction. This simple scheme was validated by our experiment. To reach up to mode (1, 4), the excitation location was located at $(x, y) = (265.879, 50.8)$ mm [$(10\frac{5}{8}, 2)$ in.] for the aluminum plate with PCLD.

A sine sweep signal was applied to the shaker with the load cell feedback to maintain the constant force magnitude for the whole frequency spectra. We set up the control voltage in the input of the load cell, and the output voltage to shaker was adjusted based on the feedback control algorithm integrated in the SigLab signal acquisition system (Spectral Dynamics, Inc.).

Results

In this section, we show the results of frequency, mode shape functions, and frequency-response function for the plate with PCLD treatment. The first 16 plate bending and in-plane mode shapes were solved and used in our analysis.[13] The material constant for Young's modulus was 68 GPa and Poisson's ratio was assumed as $\nu = 0.3$. The viscoelastic core was working under room temperature, at 20°C.

In analysis 1, a total of 25 modes, for each of five displacements, $w(x, y, t)$, $u_1(x, y, t)$, $v_1(x, y, t)$, $u_3(x, y, t)$, and $v_3(x, y, t)$, were included to achieve the frequency convergence compared to experimental results. Also three minioscillators were used to curve fit the complex shear modulus of viscoelastic material in the GHM

Table 2 Bending frequency results for a plate with PCLD treatment

		Analysis 1[a]		Analysis 2[b]	
Bending mode	Experiment, Hz	Model, Hz	Error, %	Model, Hz	Error, %
1,1	83.1	87.7	5.54	87.8	5.66
1,2	104.91	107.92	2.87	108.02	2.96
1,3	218.9	220.82	0.88	220.74	0.84
2,1	234.2	241.9	3.29	241.17	2.98
2,2	277.8	286.28	3.06	285.59	2.81

[a]Analysis 1, 25 modes for each displacement assumed leading to 500 degrees of freedom.
[b]Analysis 2, 16 modes for each displacement leading to 320 degrees of freedom.

Table 3 Loss factor results for a plate with PCLD treatment

		Analysis 1[a]		Analysis 2[b]	
Mode	Experiment	Model	Error, %	Model	Error, %
1,1	0.06	0.0448	−25.3	0.0486	−19
1,2	0.0412	0.0334	−18.9	0.0371	−9.96
1,3	0.0424	0.0275	−35.1	0.0304	−28.1
2,1	0.031	0.0302	−2.58	0.0328	5.81
2,2	0.0334	0.0297	−11.1	0.039	16.8

[a]Analysis 1, 25 modes for each displacement assumed leading to 500 degrees of freedom.
[b]Analysis 2, 16 modes for each displacement used leading to 320 degrees of freedom.

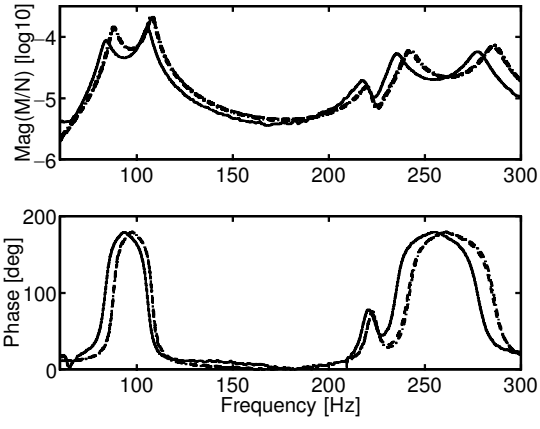

Fig. 8 Frequency response functions of a plate with PCLD, at location 11: ——, experiment; – – –, analysis 2; and –·–, analysis 1.

method. Therefore, this will triple the degrees of freedom, resulting in a model with 500 degrees of freedom. In analysis 2, for each displacement, the first 16 modes were included, which led to a model with 320 degrees of freedom.

As shown in Table 2, the frequency predictions for the first five modes in both analyses were compared to the experimental results. The largest error was in the first mode for both analyses, and both analyses achieved the same accuracy of frequency predictions. Table 3 shows the loss factors predicted by both analyses, and they are compared to the experimental data.

The experimental mode shape functions calculated using the STAR software[20] were plotted in contour form and are shown in Fig. 6. The analytical mode shape functions were plotted in Fig. 7, as well, to compare with the experimental results. Except for the modes (1, 1) and (2, 1), the mode shape functions match each other between the experimental and analytical results. The frequency-response functions predicted by analysis 1 and analysis 2 were plotted and compared against the experimental data at location 11, as shown in Fig. 8. The analytical predictions captured the general trend of the frequency-response functions for the plate with PCLD treatment, and both magnitude and phase were correlated to the experimental results.

Conclusions

For a plate with PCLD treatment, we developed two analyses, and the GHM method was incorporated to account for the frequency-dependent complex shear modulus in both analyses. The first analysis used one-dimensional beam and rod modes for all of the displacements in the assumed modes method. We included the first 25 modes for each displacement, which led to a system with about 500 degrees of freedom. The second analysis was to use two-dimensional plate bending and in-plane modes for the base plate structure, but only one-dimensional rod modes were applied to in-plane motion of the constraining plate. Our goal was to reduce the number of modes included in the assumed mode method and to maintain the accuracy of our predictions. Therefore, we developed analysis 2, in which we updated assumed modes for the base plate using plate bending and in-plane modes that were solved based on the Kantorovich–Krylov method,[9] and we used one-dimensional rod modes to approximate the in-plane displacements in the constraining plate. In analysis 2, only the first 16 modes for each displacement are included, and this leads to a system with about 320 degrees of freedom.

The computed results of frequency, mode shapes, and frequency response have been validated by the experimental results. For the natural frequency predictions, as shown in Table 2, both analyses exhibit the same accuracy compared to the experimental results. The largest error was in the first mode for both analyses, which is due to boundary condition effects. However, the computational cost was substantially reduced compared to 320 degrees of freedom in analysis 2 and 500 degrees of freedom in analyses 1.

Table 3 shows the loss factors predicted by both analyses, and they are compared to the experimental data. The errors in loss factor predictions were large but reasonable for damping predictions in a lightly damped (<5%) structure. However, we found that both analyses predicted comparable levels of damping capacity in this sandwich plate structure. The analytical damping predictions were lower than the experimental data because we cannot include all of the damping mechanism in our analyses. In analysis 2, the damping predictions were generally higher than those predicted with analysis 1.

The experimental and analytical mode shape functions for the sandwich plate were plotted in Figs. 6 and 7. There are differences between analytical and experimental results for modes (1, 1) and (2, 1). This could be the experimental errors or some other issues. We can possibly improve the mode shape measurements using a laser vibrometer to scan the entire plate.

The frequency-response functions predicted by both analyses captured the trend of experimental results measured at a point, as shown in Fig. 8. Therefore, our proposed assumed modes method can predict the behaviors of the plate with PCLD treatment with smaller computational cost compared to previous approaches using one-dimensional beam and rod mode shape functions.

Acknowledgments

Research supported by U.S Army Research Office under the FY96 Multidisciplinary University Research Initiative in Active Control of Rotorcraft Vibration and Acoustics. (G. Anderson and T. Doligalski, Technical Monitors). Laboratory equipment support was provided under the FY96 Defense University Research Instrumentation Program Contract DAAH-0496-10301 (G. Anderson, Technical Monitor). D.-C. Chang is supported in part by National Science Foundation Grant DMS9622249 and a William Fulbright Research Grant.

References

[1]Ross, D., Ungar, E. E., and Kerwin, J., "Damping of Plate Flexural Vibrations by Means of Viscoelastic Laminate," *Structural Damping*, edited by J. E. Ruzicka, American Society of Mechanical Engineers, New York, 1959, pp. 49–88.

[2]Rao, Y. V. K. S., and Nakra, B. C., "Vibrations of Unsymmetrical Sandwich Beams and Plates with Viscoelastic Cores," *Journal of Sound and Vibration*, Vol. 34, No. 3, 1974, pp. 309–326.

[3]Cupial, P., and Niziol, J., "Vibration and Damping Analysis of a Three-Layered Composite Plate with a Viscoelastic Mid-Layer," *Journal of Sound and Vibration*, Vol. 183, No. 1, 1995, pp. 99–114.

[4]Wang, G., Veeramani, S., and Wereley, N. M., "Analysis of Sandwich Plates with Isotropic Face Plates and a Viscoelastic Core," *Journal of Vibration and Acoustics*, Vol. 122, No. 3, 2000, pp. 305–312.

[5]McTavish, D. J., and Hughes, P. C., "Finite Element Modeling of Linear Viscoelastic Structures: The GHM Method," AIAA Paper 92-2380, April 1992.

[6]Doyle, J., *Wave Propagation in Structures,* Spring-Verlag, Berlin, 1997, pp. 198–242.

[7]Leissa, A., *Vibration of Plates*, Acoustical Society of America, Melville, NY, 1993: reprint of NASA SP-160, 1969, pp. 41–160.

[8]Graff, K. F., *Wave Motion in Elastic Solids*, Clarendon, Oxford, 1975, pp. 435–458.

[9]Kantorovich, L. V., and Krylov, V. I., *Approximate Methods of Higher Analysis*, Noordhoff, Groningen, The Netherlands, 1964, pp. 241–357.

[10]Washizu, K., *Variational Methods in Elasticity and Plasticity*, Pergamon, Oxford, 1968, pp. 152–181.

[11]Inman, D. J., *Engineering Vibration*, Prentice–Hall, Englewood Cliffs, NJ, 1994, pp. 437–488.

[12]Bhat, R. B., Singh, J., and Mundkur, G., "Plate Characteristic Functions and Natural Frequencies of Vibration of Plates by Iterative Reduction of Partial Differential Equation," *Journal of Vibration and Acoustics*, Vol. 115, No. 2, 1993, pp. 177–181.

[13]Wang, G., "Analyses of Sandwich Beams and Plates Structures with Viscoelastic Cores," Ph.D. Dissertation, Dept. of Aerospace Engineering, Univ. of Maryland, College Park, MD, Dec. 2001.

[14]Wang, G., and Wereley, N. M., "Free In-Plane Vibration of Rectangular Plates," *AIAA Journal*, Vol. 40, No.5, 2002, pp. 953–959.

[15]Chang, D. C., Wang, G., and Wereley, N. M., "A Generalized Kantorovich Method and Its Application to Free In-Plane Plate Vibration Problem," *Applicable Analysis*, Vol. 80, No. 3, 2002, pp. 493–523.

[16]Farag, N. H., and Pan, J., "Modal Characteristics of In-Plane Vibration of Rectangular Plates," *Journal of the Acoustical Society of America*, Vol. 105, No. 6, 1999, pp. 3295–3309.

[17]Flugge, W., *Viscoelasticity*, Blaisdell, Waltham, MA, 1969. Chap. 4.

[18]Fowler, L., Buchner, S., and Ryaboy, V., "Self-Contained Active Damping System for Pneumatic Isolation Table," *Proceedings of SPIE—The International Society for Optical Engineering Conference on Smart Structures and Integrated Systems*, Newport Beach, CA, Paper SPIE-3391-33, 2000.

[19]"ScotchDamp Vibration Control Systems," Product Information and Performance Data, 3M, St. Paul, MN, 1993.

[20]STAR System Manuals, Reference Manual 3405-0114, Spectral Dynamics, Inc., Nov. 1994.

A. Berman
Associate Editor